AIP | Journal of Applied Physics

Improvement of field emission from screen-printed carbon nanotubes by He/(N2,Ar) atmospheric pressure plasma treatment

S. J. Kyung, J. B. Park, J. H. Lee, and G. Y. Yeom

Citation: J. Appl. Phys. **100**, 124303 (2006); doi: 10.1063/1.2402966
View online: http://dx.doi.org/10.1063/1.2402966
View Table of Contents: http://jap.aip.org/resource/1/JAPIAU/v100/i12
Published by the American Institute of Physics.

JOURNAL OF APPLIED PHYSICS **100**, 124303 (2006)

Improvement of field emission from screen-printed carbon nanotubes by He/(N_2,Ar) atmospheric pressure plasma treatment

S. J. Kyung, J. B. Park, J. H. Lee, and G. Y. Yeom[a]
Department of Advanced Materials Science and Engineering, Sungkyunkwan University, Jangan-Gu, Chunchun-Dong 300, Suwon 440-746, South Korea

(Received 30 August 2006; accepted 12 October 2006; published online 19 December 2006)

A screen-printed carbon nanotube (CNT) paste for applications to field emission emitters was treated with He, He/Ar, and He/N_2 atmospheric pressure plasmas. The effect of the different plasma treatments on the field emission characteristics of the screen-printed CNTs was investigated. The atmospheric pressure plasma applied to the screen-printed CNT paste for 10 s resulted in a reduction in the turn-on electric field. In particular, the application of a He/N_2 plasma treatment decreased the turn-on electric field from 3.13 to 1.29 V/μm and increased the field enhancement factor from 737 to 2775 after the treatment. These results suggest that an adequate atmospheric pressure plasma treatment of screen-printed CNTs can be effective in enhancing the field emission properties. © *2006 American Institute of Physics*. [DOI: 10.1063/1.2402966]

I. INTRODUCTION

Carbon nanotubes (CNTs) have attracted considerable interest on account of their remarkable properties, such as their high aspect ratio, high mechanical strength, chemical stability, superthermal conductivity, and electron emission properties.[1–3] Because CNTs show extremely high electron emission currents at low operating voltages due to their high aspect ratio, CNTs are considered to be strong candidate materials for field emission displays.

Recently, a screen-printed CNT paste was used as an array for field emitters on a metallic electrode. The CNT paste film made by screen printing has advantages such as low cost and simplicity when used for large displays. However, in a screen-printed CNT paste, the poor electron emission due to entangled CNT bundles and the lack of CNTs protruding from the paste surface are some of the critical problems. Therefore, several surface treatments such as adhesion taping, soft rubber rolling, ion irradiation, low-pressure plasma exposure, etc., have been used to improve the electron emission properties of the screen-printed CNT paste films.[4–7] Among these methods, adhesive taping and soft rubber rolling are simple methods for removing the paste material mixed with the CNTs. However, these methods tend to leave an uneven residue and destroy the CNT patterns, which can result in nonuniform emission sites. In the case of ion irradiation and low-pressure plasma exposure, the processing cost is high due to the need for vacuum processing as well as difficulties in achieving large area processing.

As a possible solution for the above mentioned problems related to screen printing, this study developed an atmospheric pressure plasma treatment using a pin-to-plate-type atmospheric pressure plasma source and examined its effects on the CNT field emission characteristics.[8–10] It is believed that the production of low-cost CNT field emitters on a large area substrate can be realized using an in-line process if the CNT paste surface can be successfully treated with atmospheric pressure plasma.

II. EXPERIMENTAL DETAILS

The CNT paste was prepared by mixing multiwalled CNTs, a binder polymer, filler, and inorganic frits in a solvent. The multiwalled CNTs (MWCNTs) used in this study were grown by thermal chemical vapor deposition (CVD). The CNT paste, 2×2 cm^2 in size, was screen printed onto a soda-lime glass substrate that had been coated with indium tin oxide (ITO). The screen-printed CNT paste was baked in air at 120 °C for 10 min and fired at 380 °C in a N_2 environment in a conventional oven to burn out the organic binder of the CNT paste before applying the atmospheric pressure plasma.

Figure 1 shows a schematic diagram of the pin-to-plate-type atmospheric pressure plasma source used to treat the surface of the screen-printed CNTs. As shown in the figure, the top electrode, which was made of multipins, was con-

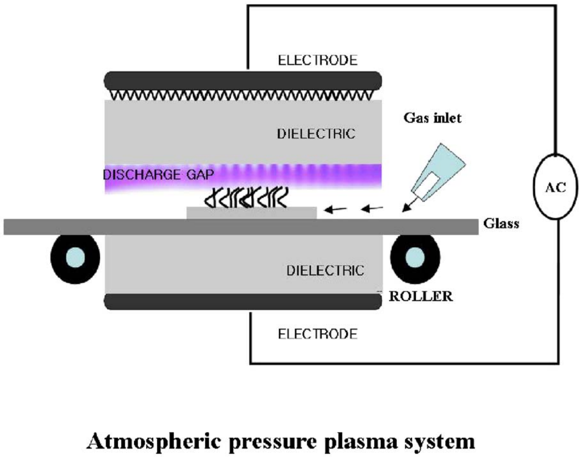

FIG. 1. (Color online) Schematic diagram of the pin-to-plate-type atmospheric pressure plasma system used in the experiment.

---

[a] Author to whom correspondence should be addressed; FAX: +82-31-299-6565; electronic mail: gyyeom@skku.edu

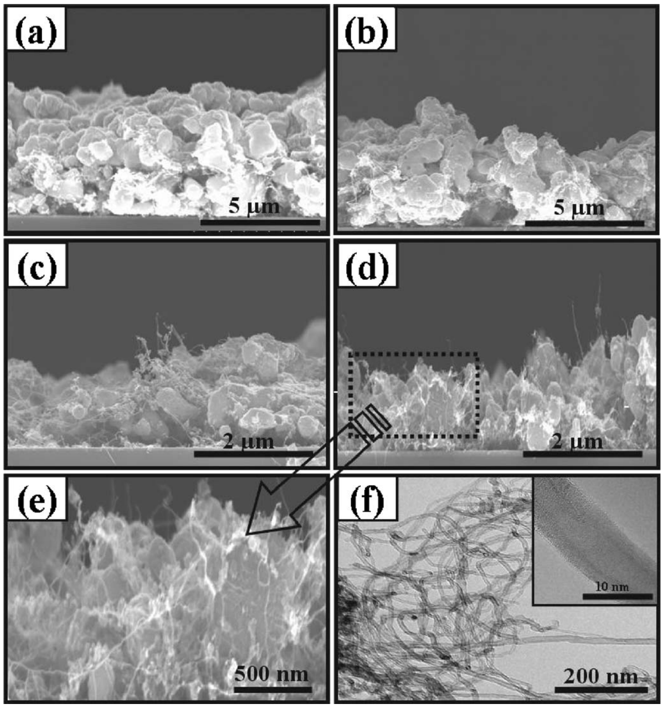

FIG. 2. SEM images of the screen-printed CNT paste (a) before, (b) after He (10 slm), (c) after He (10 slm)/Ar (0.1 slm), and [(d) and (e)] after He (10 slm)/N_2 (0.1 slm) plasma treatment for 10 s. (f) shows TEM images of MWCNTs used in the experiment for CNT paste.

nected to an ac power supply. The bottom ground electrode was a blank plate electrode (pin-to-plate type). The size of the top electrode was $1000\times 100\ \mathrm{mm}^2$. As shown in Fig. 1, on both electrodes quartz plates were located as dielectrics to limit the current flow. The air gap distance between the dielectrics of the electrodes was 4 mm. A 3–20 kV voltage power supply with a variable frequency ranging from 20 to 30 kHz was applied to the top electrode as the ac power. He (10 slm), He (10 slm)/Ar (0.1 slm), or He (10 slm)/N_2 (0.1 slm) (slm denotes standard liters per minute) was fed between the electrodes as the discharge gas. The plasma treatment time was varied from 10 to 30 s.

Transmission electron microscopy (TEM) (JEOL JEM-3011) and field emission scanning electron microscopy (FE-SEM) (Hitachi S-4700) were used to observe the CNT morphology before and after the plasma treatment. Raman spectroscopy (Renishaw RM1000-InVia) was used to observe the changes in the defects on the CNT surface after the plasma treatment. The field emission properties of the CNT field emitters before and after the plasma treatment were measured in a vacuum chamber with a parallel diode-type configuration at 2×10^{-6} Torr using a direct current (dc) power supply. The distance between the CNT field emitter and the anode was kept at 400 μm.

III. RESULTS AND DISCUSSION

Figure 2 shows SEM micrographs of the CNT paste before and after the atmospheric pressure plasma treatment using He (10 slm), He (10 slm)/Ar (0.1 slm), and He (10 slm)/N_2 (0.1 slm) for 10 s. Figure 2(a) shows the CNT paste before the plasma treatment and the CNTs covered with the remaining binder material, about 1 μm size. In this case, the CNTs were not exposed to the paste surface. Therefore, the field emission properties of the CNT paste were not good. In order to modify the surface morphology, the CNT surface was treated with the atmospheric pressure plasma of (b) He (10 slm), (c) He (10 slm)/Ar (0.1 slm), and [(d) and (e)] He (10 slm)+/N_2 (0.1 slm) for 10 s at an input voltage of 10 kV. As shown in Figs. 2(b)–2(d), after the He atmospheric pressure plasma treatment, some of the paste had been removed but there was no significant protrusion of CNTs. However, after the He/Ar or He/N_2 plasma treatment, approximately 2–3 μm more paste was removed, possibly due to the surface bombardment effect by Ar^+ and $N_2{}^+$. In addition to the increased removal of paste by the He/Ar or He/N_2 plasma treatment, it resulted in the protrusion and vertical alignment if CNTs similar to the CNTs were aligned by a vertical force during the removal of tape in the adhesive taping method. This was attributed to the removal of excessive paste and by cutting of the tangled CNTs. In particular, more CNTs appeared from the paste surface after the He/N_2 plasma treatment, as shown in Fig. 2(e). Figure 2(f) shows TEM micrographs of the long tangled multiwalled CNTs with an external diameter of approximately 10 nm.

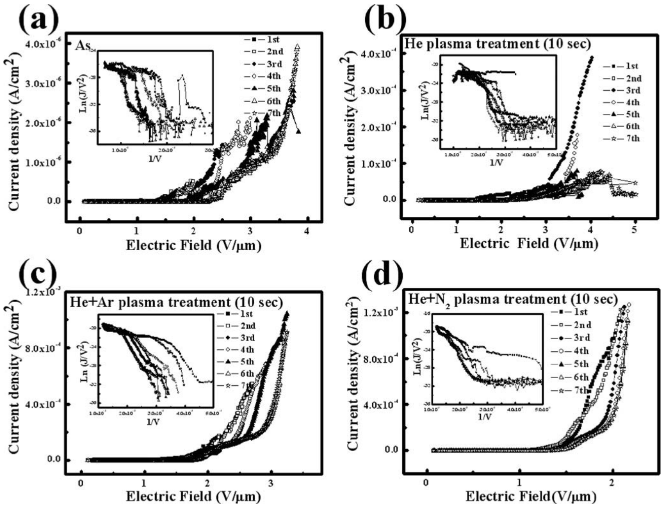

FIG. 3. Emission current density (J) vs the electric field (E) for CNTs (a) before, (b) after He (10 slm), (c) after He (10 slm)/Ar (0.1 slm), and (d) after He (10 slm)/N_2 (0.1 slm) plasma treatment for 10 s. The insets correspond to the Fowler-Nordheim (FN) plots. The E-J characteristics were measured seven times.

The field emission characteristics of the CNT paste were observed before and after the atmospheric pressure plasma treatments. Figure 3 shows the electric field (E) versus current density (J) of the CNTs (a) before the plasma treatment, (b) after the He (10 slm) plasma treatment, (c) after the He (10 slm)/Ar (0.1 slm) plasma treatment, (d) and after the He (10 slm)/N_2 (0.1 slm) plasma treatment. The field emission characteristics were measured seven times repeatedly and the effect of aging on the field emission characteristics was also investigated. The inset shown in Fig. 3 shows the Fowler-Nordheim plots of each field emission curve. The emission current density J can be expressed as the Fowler-Nordheim equation:[11–13] $J=(AE^2/\Phi)\exp(-B\Phi^{3/2}/E)$, where $A=1.54\times 10^{-6}\ \mathrm{A\ eV\ V^{-2}}$, $B=6.83\times 10^9\ \mathrm{eV^{-3/2}\ V\ m^{-1}}$, and E (the lo-

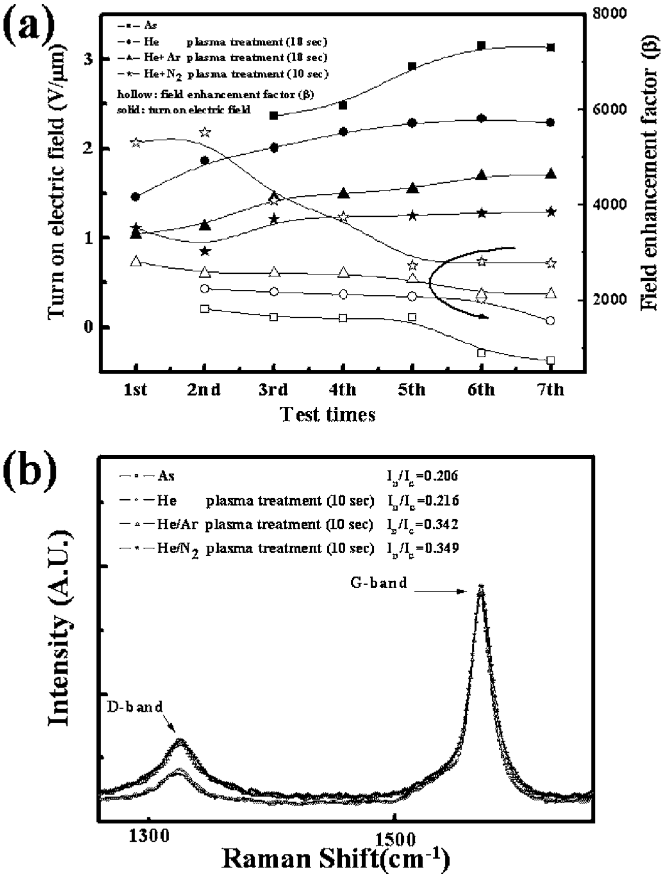

FIG. 4. Variation in the turn-on electric field and field enhancement factor for repeated measurements of *E-J*. (b) Raman spectra of the CNT emitters before and after the plasma treatments for 10 s.

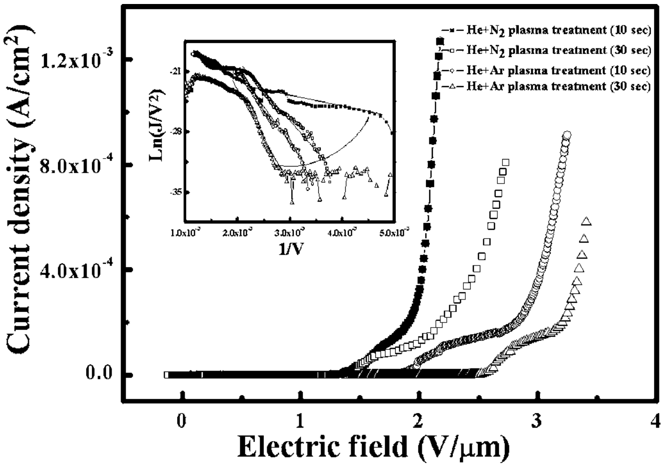

FIG. 5. Emission current density (J) vs the electric field (E) for CNT emitters after the He (10 slm)/Ar (0.1 slm) and He (10 slm)/N$_2$ (0.1 slm) plasma treatment for 10 s and 30 s. The inset corresponds to Fowler-Nordheim (FN) plots.

cal field at the emitting tip) $=\beta E_0=\beta(V/d)$. Here, β is the field enhancement factor. β was calculated from the graph of (J/E^2) vs $(1/E)$ assuming Φ (work function) of the MWCNTs to be 5 eV. The calculated field emission factors and the turn-on electric field E_{to} (defined as the electric field at 1 μA/cm^2 of the emission current density) are also shown in Fig. 4(a). As shown in Figs. 3 and 4(a), when the *E-J* characteristics were measured repeatedly, E_{to} increased and β decreased with increasing number of measurements. However, E_{to} and β became saturated with large number of measurements. For example, after the He/N$_2$ plasma treatment, E_{to} increased from 0.85 to 1.29 V/μm and β decreased from 5522 to 2775 with increasing number of measurements from 1 to 7. Indeed, the emission current of the screen-printed CNT emitters was initially unstable due to the nonuniformity of the distance between the emitter tips and the electrode.[14] In addition, the CNT emitters exposed after the plasma treatment also do not have the same length. Therefore, among the CNTs exposed on the surface, only the long CNTs emit electrons initially with a hot spot being observed. However, a more stable emission current is obtained as the long CNTs and CNTs that are loosely bonded to the surface are removed from the paste surface by the repeated measurement, in a similar manner to the aging process.

As shown in Figs. 3 and 4(a), when the *E-J* characteristics were measured, the E_{to} and β before the plasma treatment were 3.13 V/μm and 737 after the seventh measurement, respectively. However, after the He, He/Ar, and He/N$_2$ plasma treatments, the E_{to} decreased to 2.29, 1.71, and 1.29 V/μm, respectively, and β increased to 1566, 2133, and 2775, respectively, after the seventh measurement. The decrease in E_{to} and the increase in β as a result of the He, He/Ar, and He/N$_2$ plasma treatments in that order was attributed to the removal of a more paste and the resulting formation of more protruded vertical CNTs, as shown in Fig. 2. In particular, in the case of the plasma treatment by He/Ar and He/N$_2$, it is believed that the significant changes in E_{to} and β are related to the formation of defects on the CNT surface as a result of the heavy ion bombardment. In addition, in the case of the He/N$_2$ treatment, nitrogen doping into MWCNTs is believed to assist in decreasing the E_{to} and increasing the β.

The increase in the number of defects on the CNT surface after the plasma treatments was observed by Raman spectroscopy. Figure 4(b) shows the Raman spectra measured on the CNT paste before and after the plasma treatments for 10 s. As shown in the figure, the I_D/I_G ratio, where I_D/I_G is the relative peak intensity ratio of the D band (defectlike band, 1350 cm^{-1}) and G band (graphitelike band, 1580 cm^{-1}), increased from 0.206 to 0.216, 0.342, and 0.349 by the He, He/Ar, and He/N$_2$ plasma treatments for 10 s, respectively. In particular, the significant increase in I_D/I_G by the He/Ar and He/N$_2$ treatment is related to heavy ion bombardment such as Ar$^+$ and N$_2$$^+$ to the exposed CNT surface. The increase in the number of CNT surface defects by heavy ion bombardment increases the electron emission of the CNTs, which decreases E_{to} and increases β.

Figure 5 shows the effect of the plasma exposure time of 10 and 30 s on the field emission characteristics of the CNT emitters for He (10 slm)/Ar (0.1 slm) and He (10 slm)/N$_2$ (0.1 slm). As shown in the figure, E_{to} and β changed from 1.71 V/μm and 2133 to 2.45 V/μm and 1789 with increasing the He/Ar plasma exposure time from 10 to 30 s, respectively. In the case of He/N$_2$, E_{to} and β changed from 1.29 V/μm and 2775 to 1.35 V/μm and 2285, respectively. Therefore, E_{to} increased and β decreased with increasing the plasma exposure time from 10 to 30 s. The emitting current densities were also decreased by approximately 35%. The plasma treatments used in this experiment remove the paste material from the CNT paste surface, expose the CNTs, and activate the CNT surface by forming defects on the surface. However, the decrease in the field emission characteristics obtained after 30 s exposure is believed to be related to the significant decrease in the CNT emitter length and number as a result of excessive ion bombardment. More studies will be needed on the effects of various time exposures and pressures in order to fully understand the enhanced field emission properties from the screen-printed CNTs.

IV. CONCLUSIONS

In this study, screen-printed CNTs were treated with pin-to-plate-type atmospheric pressure plasma using He (10 slm), He (10 slm)/Ar (0.1 slm), and He (10 slm)/N_2 (0.1 slm) gases, and the effect of the plasma treatments on the field emission characteristics of the CNT paste was investigated. For the stable measurement of the field emission characteristics of CNT paste, repeated measurements of the *E-J* characteristics are needed until it becomes saturated as a result of the removal of hot spots. When the *E-J* characteristics after the seventh measurement were compared, the plasma treatments for 10 s showed improved field emission characteristics of the CNT paste. Among the plasma treatments, the He (10 slm)/N_2 (0.1 slm) treatment produced the lowest E_{to} and the highest β by decreasing E_{to} from 3.13 to 1.29 V/μm and increasing β from 737 to 2775. The improved field emission characteristics were attributed to the exposure of CNTs and the vertical alignment of the exposed CNTs as a result of ion bombardment from the plasma. In addition, the formation of defects on the exposed CNT surface as a result of heavy ion bombardment is related to the enhancement of field emission characteristics of the CNT emitters. However, an increase in the plasma treatment time to 30 s degraded the field emission characteristics due to the significant decrease in the CNT emitter length and number as a result of excessive ion bombardment such as Ar^+ and N_2^+. If the plasma treatment of CNT paste can be successfully applied by the atmospheric pressure plasma, it is believed that the production of low-cost CNT field emitters on a large area substrate can be achieved using an in-line process.

ACKNOWLEDGMENT

This work was supported by the National Program for Tera-Level Nanodevices of the Korean Ministry of Science and Technology as a 21st Century Frontier Program.

[1] C. Liu, Y. Y. Fan, M. Liu, H. T. Cong, H. M. Cheng, and M. S. Dressel, Science **286**, 1127 (1994).
[2] W. A. de Heer, A. Chatelain, and D. Ugarte, Science **270**, 1179 (1995).
[3] Y. H. Lee, Y. T. Jang, D. H. Kim, J. H. Ahn, and B. K. Ju, Adv. Mater. (Weinheim, Ger.) **13**, 479 (2001).
[4] T. J. Vink, M. Cillies, J. C. Kriege, and H. W. J. J. Vande laar, Appl. Phys. Lett. **83**, 3552 (2003).
[5] D. H. Kim, C. D. Kim, and H. R. Lee, Carbon **42**, 1807 (2004).
[6] Y. C. Kim, K. H. Sohn, Y. M. Cho, and E. H. Yoo, Appl. Phys. Lett. **84**, 5350 (2004).
[7] A. Gohel, K. C. Chin, Y. W. Zhu, C. H. Sow, and A. T. S. Wee, Carbon **43**, 2530 (2005).
[8] Y. H. Lee and G. Y. Yeom, Jpn. J. Appl. Phys., Part 1 **44**, 1076 (2005).
[9] S. J. Kyung, Y. H. Lee, C. W. Kim, J. H. Lee, and G. Y. Yeom, Thin Solid Films **506**, 268 (2006).
[10] A. Kuwabara, S. I. Kuroda, and H. Kubata, Plasma Processes Polym. **2**, 305 (2005).
[11] I. S. Altman, P. V. Pikhitsa, and M. S. Chio, Appl. Phys. Lett. **84**, 1126 (2004).
[12] J. T. L. Thong, C. H. Oon, W. K. Eng, W. D. Zhang, and L. M. Gan, Appl. Phys. Lett. **79**, 2811 (2001).
[13] S. J. Kyung, Y. H. Lee, C. W. Kim, J. H. Lee, and G. Y. Yeom, Carbon **44**, 1530 (2006).
[14] G. S. Choi, K. H. Son, and D. J. Kim, Microelectron. Eng. **66**, 206 (2003).